basis of the differences between bonds which are chemically equivalent and a comparison with the known dimensions of benzene rings. These estimates do not apply to the pyridine of crystallization, which appears to have very large and anisotropic thermal motion (B is about 15 to 20 $Å^2$) and which may have some kind of disorder. Average values of the lengths and angles of some chemically equivalent bonds are given in Fig. 2. We expect these average distances to have standard deviations of the order of 0.01 Å. The standard deviations of the bond angles are on the order of 1° or less. The bond distances and angles are in agreement with results on other phthalocyanines (*3*).

Each terminal pyridine (Figs. 1 and 2) is oriented so that its plane bisects two of the N—Mn—N angles of the adjacent phthalocyanato complex. One phthalocyanine ring is rotated 41° with respect to the other about the Mn—O—Mn axis so that its benzene rings are approximately between the benzene rings of the other. Except for the benzene rings the atoms of each ring system lie in a plane with the respective manganese atom. The benzene rings bend inward toward the empty spaces of the opposite half of the molecule by from 0.1 to 0.6 Å. We consider this bending to be the result of molecular packing forces in the crystal and assume it to have no chemical significance except as a reflection of the flexibility of such a large molecule.

The Mn—O distance of 1.71 ± 0.01 Å is shorter than we would have predicted for a single covalent bond. We expect that an explanation of the magnetic properties will involve electronic coupling between manganese atoms through this bond system.

The mechanisms proposed for the formation of this complex (*1, 2*) need to be reexamined in the light of this new formulation.

LESTER H. VOGT, JR.*
ALLAN ZALKIN
DAVID H. TEMPLETON
Lawrence Radiation Laboratory and
Department of Chemistry,
University of California, Berkeley

References and Notes

1. J. A. Elvidge and A. B. P. Lever, *Proc. Chem. Soc.* **1959**, 195 (1959).
2. G. Englesma, A. Yamamoto, E. Markham, M. Calvin, *J. Phys. Chem.* **66**, 2517 (1962).
3. J. M. Robertson, *J. Chem. Soc.* **1936**, 1195 (1936); ——— and I. Woodward, *ibid.* **1937**, 219 (1937); **1940**, 36 (1940).
4. All molecules in one crystal are of the same handedness, but another crystal from the same preparation is as likely to be right-handed as left-handed. Thus there is no general significance to the absolute configuration which we found.
5. One of us (L.H.V.) was NIH postdoctoral fellow. We thank Prof. Calvin for bringing this very interesting substance to our attention. Partly supported by AEC.
* Present address: General Electric Research and Development Center, K-1, P.O. Box 8, Schenectady, N.Y. 12301.

13 December 1965

Distribution of Uranium in Some Natural Minerals

Abstract. *The advantages of the fission method over conventional autoradiography for studying the distribution of uranium in natural minerals is described. Relatively high concentrations of uranium associated with micro inclusions in the St. Marks enstatite chondrite have been observed and may account for the variation of the uranium concentrations in different samples of this meteorite.*

In order to study the distribution of uranium in various natural silicates by the fission method (*1*) a 700-million-year-old mica was selected as the detecting medium. An etching time of 40 minutes and 48 percent HF were used, which permitted removal of any surface contamination. After neutron irradiation, no clusters of tracks were seen, so that the mica was well-suited for localizing areas of uranium enrichment in the samples. The samples consisted of uncovered thin sections of rocks which were fixed to either plastic or silica mounts. After neutron irradiation, common minerals present in the sample can be arranged in order of decreasing uranium concentration as follows: accessory minerals, biotite, potassic feldspar, amphibole, pyroxene, olivine, and quartz. Exceptions to the sequence were observed, particularly in amphibole and quartz. In fine-grained volcanic rocks and granites that had been altered by pneumatolysis, uranium was often concentrated along intercrystal areas (Fig. 1, left). Accessory minerals, such as apatite from a ferrogabbro (Fig. 1, center), showed a fairly even distribution of tracks compared to sphene (Fig. 1, right) which shows the enrichment of uranium in some areas of the crystal.

The fission-track method has the distinct advantage over autoradiographic methods in that, for very small amounts of uranium, many tracks can be induced simply by increasing the irradiation exposure time.

Meteorites are known to contain very small amounts of total uranium, but zircon and the phosphate mineral, whitlockite (*2*), containing high concentrations of uranium, have been found in the Vaca Muerta (*3*) mesosiderite.

I have investigated the quartz-bearing enstatite chondrite St. Marks (*4*). After thermal neutron irradiation and etching, 95 percent of the exposed meteorite surface contained no significant track populations above the general track background. In one area of the sample, covering about 0.2 cm^2, a very high population of tracks was present; this suggested that the tracks were the mirror images of small uranium-bearing minerals. In Fig. 2*a*, a rectangular area of tracks forming a rim enclose a clear area which, in turn, contains a high-density spot in the center; in Fig. 2*b* the tracks clearly outline three sources having prismatic forms. In the same area of the sample, a high-density track population was associated with well-defined "sunbursts" (Fig. 2*c*), which Price and Walker (*1*) have related to surface contamination by dust that contained uranium. The spatial distribution of these tracks is a result of the passage of a fission fragment through air before being registered at the detecting mica surface.

I accept the interpretation of this feature, but in the study I present here, in which twenty thin sections of rock were examined, the "sunbursts" were associated with the meteorite sample, and this suggests some direct relation with the sample. To study this further, the sample was carefully washed in hot dilute nitric acid and boiled in demineralized water (distilled in quartz) for 15 minutes. The sample was then irradiated for a second time and, after etching, continued to show "sunbursts" in the same area, fewer in number and more dispersed, as shown in Fig. 2*d*; these samples were photographed at a lower magnification and etched for a

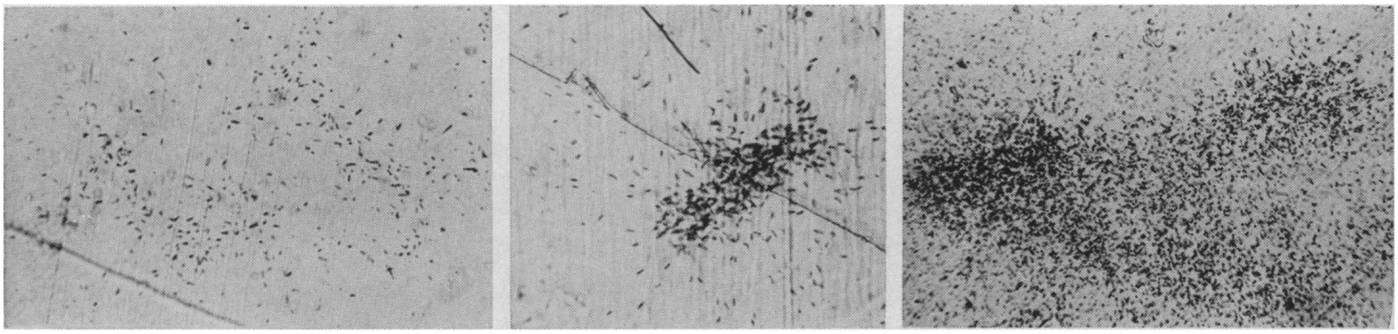

Fig. 1. Induced fission tracks in minerals. (Left) The distribution of uranium in areas of intercrystal devitrified glass between the major minerals; alkali basalt, Hawaii (uranium ~ 15 ppm). (Center) Distribution of uranium in a prismatic section of apatite; EG 4312 ferrogabbro, Skaergaard intrusion, E. Greenland. The distribution of tracks around the crystal may be the result of local "contamination" caused by the presence of small fragments of apatite (~ 10 ppm of uranium). (Right) The heterogenous distribution of uranium in a section of sphene; Ross of Mull granite, Scotland (~ 250 ppm of uranium).

longer time in order to produce more intense tracks. The continued registration of tracks from the same area of the section would not appear to be compatible with accidental surface contamination. Other possibilities to account for this feature are as follows:

1) Sunbursts could be produced by the projection of a hard mineral, such as zircon, above the general plane of the section, or a soft or brittle mineral which would be shattered during polishing; and by fragments embedded in the surrounding area.

2) The general dispersion of the track population after acid treatment would be in keeping with the partial decomposition of a soluble mineral followed by a local smearing over adjacent areas. Among the minerals recorded in meteorites, the most obvious choice would be one of the phosphates such as apatite [$Ca_5(PO_4)_3Cl_1$], whitlockite [$Ca_3(PO_4)_2$], merrillite [$Na_2Ca_3(PO_4)_2$-O], or farringtonite [$Mg_3(PO_4)_2$] which, after acid treatment, would produce a gelatinous hydrated phosphate.

3) Contamination introduced into the meteorite after its fall is another possibility. Some experiments indicate that the sample is very porous and groundwater containing relatively more uranium could penetrate and become fixed on ferric oxides. Alternatively, a contaminant containing uranium could become embedded during cutting and polishing.

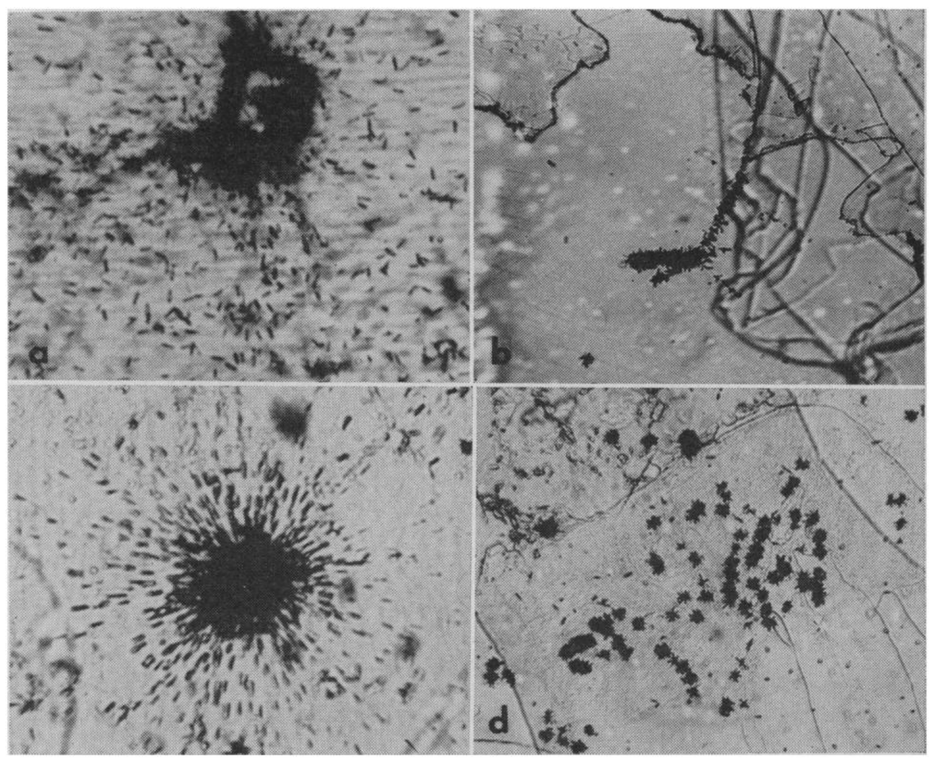

Fig. 2. The distribution of fission tracks in the St. Marks meteorite. (*a*) High concentration of tracks, possibly representing a cross section of zircon; (*b*) tracks originating from three prismatic sources; (*c*) typical sunburst pattern of tracks; (*d*) track distribution after acid treatment. Track lengths about 10 μ.

Previous uranium measurements on St. Marks (*5*) have established either that this meteorite has been contaminated with uranium or that its uranium content is variable by more than a factor of 10 from sample to sample. The present study indicates that uranium is not homogenously distributed throughout the meteorite. The presence of uranium-enriched accessory minerals presents a formidable problem in sampling which should also be reflected in measurements of zirconium. The presence of a fairly soluble uranium-rich phosphate mineral can, through the agency of natural weathering processes, result in a heterogenous redistribution of uranium together with loss of uranium through leaching.

The fission track method offers the only means for studying the distribution and concentration of uranium at very low concentrations. Early studies indicate that it is possible to apply the isochron technique of dating by measuring the ratio of spontaneous to induced fission tracks in various minerals of the same rock sample that contain differing concentrations of uranium.

E. I. HAMILTON*

Department of Geology and Mineralogy, Oxford University, Oxford, England

References and Notes

1. P. B. Price and R. M. Walker, *J. Geophys. Res.* **68**, 16, 4847 (1963); R. L. Fleischer and P. B. Price, *Geochim. Cosmochim. Acta* **28**, 1705 (1964).
2. R. L. Fleisher, C. W. Naeser, P. B. Price, R. M. Walker, U. B. Marvin, *Science* **148**, 629 (1965).
3. U. B. Marvin and C. Klein, Jr., *ibid.* **146**, 919 (1964).
4. Provided by Dr. T. H. Barry, Director, South African Museum (Natural History), Cape Town.
5. G. Anders, *Geochim. Cosmochim. Acta* **26**, 723 (1962).

* Present adress: Radiological Protection Service, Belmont, Sutton, England.

25 October 1965

Structure and Organization of the Living Mitotic Spindle of Haemanthus Endosperm

Abstract. *New details of mitotic spindle structures in the endosperm of* Haemanthus katherinae *(Bak) have been demonstrated by differential interference microscopy. Spindle fibers are clearly seen in the living spindle extending from the kinetochores to the polar region. Individual spindle fibers consist of a bundle of smaller filaments which diverge slightly from the kinetochore and intermingle with filaments from other spindle fibers as they approach the polar region. The degree of intermingling increases during metaphase and anaphase. The chromosomes stop moving when the spindle fibers are still 5 to 10 microns long; then the fibers disappear. These observations explain some aspects of spindle movements which were difficult to reconcile with earlier concepts of spindle organization.*

Although spindle fibers were depicted by cytologists of the last century (*1*) from studies on fixed and stained material, these fibers were probably not seen in normal living cells until Cooper (*2*) observed them in the division of the blastomeres of a mite, with the bright-field microscope. The early work of Inoué (*3*) established that the spindle contains birefringent, longitudinal bands that have been assumed to be equivalent to spindle fibers seen in fixed cells. Since that time, polarized light microscopy has been the method of choice for study of the living mitotic spindle.

Some years ago, Bajer and Molè-Bajer (*4*) introduced a promising new material for the study of mitosis, the endosperm of *Haemanthus katherinae* (Bak). Nuclei of these cells (or syncytia in the earlier development of the endosperm) are large and give rise to 27 chromosomes ($N = 9$), the largest of which are about 100 μ long in late prophase. In flattened cells, the mitotic spindle is often nearly 70 μ long and the equatorial plate 100 μ wide (*5*). In a series of studies, the motions of chromosomes and other particles in and on the spindle have been recorded by frame-by-frame analysis of phase-contrast time-lapse films (*6*). *Haemanthus* endosperm is probably the best plant material now available for studies of the details of chromosome movement during mitosis.

Haemanthus endosperm is also an ideal material for the study of spindle structure, organization, and function, but spindle fibers are seldom seen in living cells except under polarized light, and least of all in cells that go on to divide. One of us has reported (*7*) that of several hundred cells observed with phase-contrast optics, in only about 5 percent that divided in a perfectly normal way were spindle fibers clearly observed.

The invisibility of the spindle fibers of most dividing cells with sensitive phase-contrast or interference microscopes has been interpreted in the past (*8*) as indicative of insufficient difference in optical path because of a good refractive-index match between the fibers (if they exist as seen in fixed and stained material) and their matrix. It occurred to one of us (R.D.A.) that another explanation might be the inherent insensitivity of phase-contrast microscopes under the conditions in which spindle fibers are looked for. (Spindle fibers may be considered as thin, linear structures lying side by side in the plane of focus so that each is partially obscured by its neighbors' halos; in addition, particulate and fibrillar structures above and below their plane of focus contribute phase disturbances that degrade the image.)

We therefore undertook a joint preliminary examination of dividing *Haemanthus* cells in the Nomarski differential interference contrast system (*9*) [hereafter referred to as the Nomarski system (*10*)].

The detail that can be observed in the cover photograph and in Figs. 1–3, which show the same cell at later stages, readily attests to the elegance of the Nomarski system for the investigation of the living mitotic spindle. Comparison of Fig. 1*a* (phase contrast) and 1*b* (Nomarski system) immediately shows a wealth of detail in Fig. 1*b* that is either missing from the phase-contrast photograph or partly obscured by phase disturbances above and below the plane of focus. Most noteworthy are the readily distinguished fibrillar elements in the spindle and the substructure visible in the chromosomes.

The image obtained with the Nomarski system and other differential interference contrast microscopes deserves brief explanation, since this class of instruments may be unfamiliar to many readers. The "optical shadow-casting effect" in the image is not caused by any kind of anaxial illumination, nor is it to be interpreted as a representation of a third dimension. Instead, the distribution of brightness in the image of, for example, a spindle fiber corresponds to the derivative of the brightness distribution that would be observed in an ordinary interference microscope with bias compensation. Thus, instead of the contrast being all negative or all positive, depending on the bias compensation, as in normal interference contrast (*11*), the contrast appears sharpest where the rate of change in optical path is greatest; it is positive on one side of the object and negative on the other. The effect, therefore, is as of a "shadow"—almost as if side lighting were used—but the direction from which the shadow is cast depends upon the analyzer setting and on whether the object is phase-advancing or phase-retarding relative to its immediate surround. Since the optical system makes use of a very small lateral optical shearing, the system has a fixed directionality. Therefore, objects lacking spherical symmetry must be rotated on the stage to reveal different features of interest. An important characteristic of the Nomarski system is relative freedom from phase disturbances from structures above and below the plane of focus. Thus, at high working apertures, the field is quite shallow. The system uses polarized light to effect its beam separation, and therefore birefringence is visible if sufficiently strong. However, the spindle fibers observed in the present study were resolved as refracting rather than as birefringent bodies.

Several new findings about the structure and organization of the *Haemanthus* spindle have emerged from only these preliminary observations and photographs taken with the Nomarski system.